SAND2021-2573J

Multi-component and multi-phase lipid nanotubes formed by gliding microtubule-kinesin motility and Phase-Separated Giant Unilamellar Vesicles

Zachary I. Imam and George D. Bachand

Center for Integrated Nanotechnologies, Sandia National Laboratories, Albuquerque, NM 87185

E-mail: gdbacha@sandia.gov

Abstract

Cytoskeletal filaments and motor proteins are critical components in the transport and reorganization of membrane-based organelles in eukaryotic cells. Previous studies have recapitulated the microtubule-kinesin transport system *ex vivo* to dynamically assemble large-scale nanotube networks from multilamellar liposomes and polymersomes. Moving toward more biologically relevant systems, the present work examines whether lipid nanotube (LNT) networks can be generated from giant unilamellar vesicles (GUVs) and subsequently characterizes how the lipid composition may be tuned to alter the dynamics, structure, and fluidity of networks. Here, we describe a two-step process in which microtubule motility (*i*) drives the transport and aggregation of GUVs to form structures with a decreased energy barrier for LNT formation, and (*ii*) extrudes LNTs without destroying parent GUVs, allowing for the formation of large LNT networks. We further show that the lipid composition of the GUV influences formation and morphology of the extruded LNTs and associated networks. For example, LNTs formed from phase-separated GUVs (e.g., liquid-solid phase-separated, and coexisting liquid-ordered and liquid-disordered phase-separated) display morphologies related to the specific phase behavior reflective of the parent GUVs. Overall, the ability to form nanotubes from compositionally complex vesicles opens the door to generating lipid networks that more closely mimic the structure and function of those found in cellular systems.

Introduction

Dynamic reorganization of reticulated membrane-based organelles by cytoskeletal motor proteins and filaments is integral for basic cellular function.[1] These processes are driven by the conversion of chemical energy to mechanical work performed by biomolecular machines and enables lipid membranes to adopt morphologies that are far from thermodynamic equilibrium. In turn, cells use these membrane structures to create interconnected networks for the direct diffusive and osmotic transport of proteins,[2] nucleic acids,[3] and other molecules.[4] For example, membranous tubules formed in organelles such as the endoplasmic reticulum (ER) and Golgi apparatus are vital for their function as the main hubs for lipid and protein synthesis and transport within the cytosol.[5, 6] Membranous tubules, specifically, tunneling nanotubes,[1] have also been observed between cells and implicated in cell-to-cell communication and transport of cargos (e.g., proteins, organelles, and viruses)[4] in multiple cell types including neuronal cells,[7] immune cells,[8] and some cancer cell lines.[9] These reports suggest that dynamic lipid structures are instrumental to a wide range of biological and cellular processes but remain a nascent area of study with the potential to impact our understanding of cellular communication and disease pathologies that involve such lipid structures.

Membrane-bound organelles are largely composed of different types of glycerophospholipids, which are amphiphilic biomolecules that typically organize into fluid bilayer membranes. The exact membrane composition is dependent on the specific organelle and ultimately relate to the organelle's function. The membranes of the ER and Golgi apparatus, for example, are composed of different ratios of lipid species including saturated lipids, unsaturated lipids, and cholesterol.[10] These biomolecules spontaneously assemble *in vitro* to form equilibrium structures such as micelles,[11] vesicles,[11] and planar bilayers,[12] which have been broadly studied as biophysical models of cell membranes[13] as well as applications in drug and gene delivery.[14] At biologically relevant temperatures, lipid membranes exhibit *in vitro* changes

in their phase behavior, including the sequestration of saturated lipids and cholesterol into small (nanoscale) phase domains to drive membrane reorganization for cellular processes.[15, 16] The deliberate formation and dynamic reorganization of nonequilibrium lipid structures (e.g., tubules) that mimic biological structures such as the ER and Golgi apparatus, however, has remained challenging.

The study of *ex vivo* lipid tubules necessitates a model system in which mechanical forces may be to overcome thermodynamic barrier limiting the formation of tubule structures. Here, lipid nanotubes (LNTs) have been extruded from cells and man-made lipid vesicles using optical tweezers,[17] micropipettes,[18] and motor proteins,[19, 20] and used to characterize microfluidic transport and communication, and mechanisms of cellular analyte transport and cellular signaling pathways. As an example, using the inverted (gliding) motility assay (IMA), large-scale LNT networks were generated using kinesin motor proteins, microtubules, and multi-lamellar vesicles (MLVs).[21] In this system, kinesin motors powered by chemical energy from ATP provided the work necessary to overcome the energetic barrier to extrude LNTs and drive the dynamic organization of complex networks of LNTs. Briefly, biotinylated microtubules are propelled across a kinesin-coated surface in the IMA. The introduction of streptavidin and biotin-containing MLVs enabled non-covalent binding among the microtubules and MLVs, and the motion of the microtubules drives extrusion of LNTs from the large reservoir of lipid membrane in the MLVs. The LNT networks morphologically exhibited surface densities and network branching similar to those of the ER and Golgi apparatus. These networks were in turn used to study diffusive transport on the outer surface of the LNTs, demonstrating single-file 1D diffusion of nanoparticles and localized confinement dependent on nanoparticle density.[21]

LNT networks generated from MLVs are relatively restricted in their biological relevance based on their simple lipid formulation, generally consisting of only unsaturated lipids. As such, the use of kinesin

motors combined with lipid vesicles comprised of multiple lipid species represents a potential model system to study the biophysical properties of compositionally complex LNTs that more closely mimic their biological analogs. Giant unilamellar vesicles (GUVs) are a commonly used tool to study lipid membrane biophysics and can be reliably fabricated with complex lipid formulations to study lipid phase behavior,[13] lipid membrane mechanics,[22] and protein-lipid interactions.[23] Extrusion and fission of LNTs from GUVs have previously been described using biomolecular motors in the standard (i.e., cellular) motility geometry.[19, 20] In the present work, we hypothesized that large-scale LNT networks could be dynamically assembled using the kinesin IMA and GUVs, and that the morphological properties may be tuned with complex lipid formulations. The assembly of LNT networks is described by a two-step process in which kinesin-transport induces the aggregation of GUVs, followed by the extrusion of LNTs, forming large-scale, high-reticulated networks. Altering the lipid composition of the GUVs further enables the observation of changes in the physical characteristics as well as phase separation in LNTs. Overall, these results represent a key first step towards the study of compositionally complex lipid tubules that more closely mimic the structures and functions of those found in cellular systems.

Results and Discussion

Extrusion of Lipid Nanotube Networks (LNT) from GUVs

Large, complex networks of lipid and polymer nanotubes were formed using MLVs combined with the kinesin-microtubule IMA, demonstrating that the size and morphology of networks could be tuned by changing the microtubule density, concentration of ATP (i.e., energy), and the amount and the intrinsic fluidity of the lipid membrane.[21, 24] Networks formed from MLVs with simple lipid formulations, however, are of limited biological relevance as their cellular analogs (e.g., ER and Golgi apparatus) are comprised of multiple lipid species including sphingolipids, cholesterol, and phospholipids such as phosphatidylcholine (PC), phosphatidylethanolamine (PE), phosphatidylserine (PS), and

phosphatidylinositol (PI).[10] Moving toward a more biological relevant system, we used kinesin motility and GUVs with complex lipid formulations to form LNT networks and examine how composition may be altered to study membrane phase separation and tune the properties of LNTs.

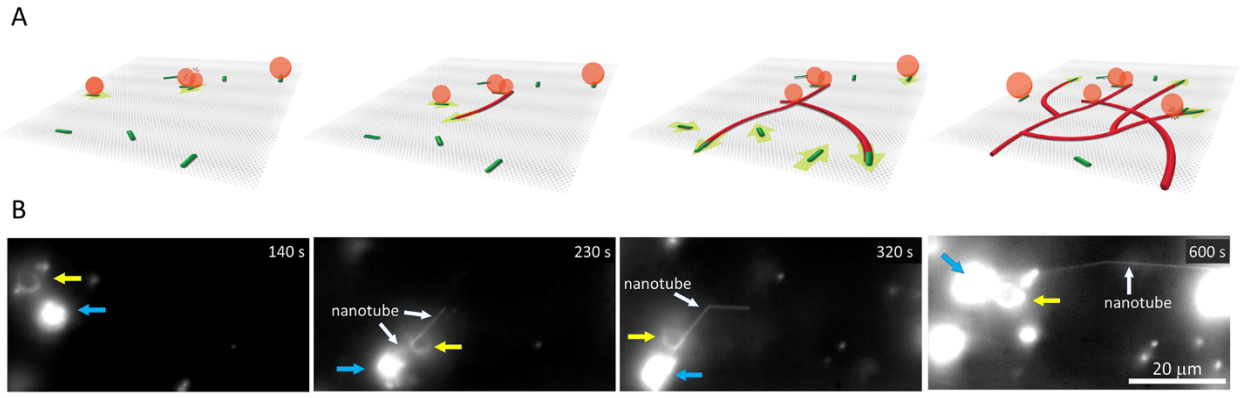

Figure 1. Microtubule Transport Induces Aggregation of GUV and Extrusion of LNT Networks. (A) GUVs (red) are bound to and transported by biotinylated microtubules (green), leading to collisions among GUVs and the formation of aggregates (first panel). The aggregates provide a lipid reservoir from which LNTs are extruded by microtubules pulling in opposing directions on the aggregated GUVs (second panel). Intersecting and branched LNTs are observed as the microtubules continue acting the GUVs and LNTs (third and fourth panel). (B) Time-lapse fluorescence images where two GUVs (yellow and blue arrows) are pulled together, resulting in the formation of an LNT. The GUVs are transported by microtubules (not visible in these images) and collide, forming an aggregate at t= 140 s. A nanotube forms between the two vesicles and a second nanotubes is extruded (t= 230s) and continues to be extended (t= 320 s) until it connects to another GUV aggregate (t = 600 s).

Our initial goal was to determine whether the kinesin IMA could support the formation of LNT networks from single lipid component GUVs. While extrusion of individual LNTs from GUVs was previously observed using membrane-bound kinesin motors moving along surface-tethered microtubules,[19, 20, 25] the resulting LNTs did not exhibit extensive lengthening or branching comparable to those formed using

MLVs and the IMA.[21, 24] In the present work, we introduced GUVs composed of 95% 1,2-dioleoyl-*sn*-glycero-3-phosphocholine (DOPC) and 5% 1,2-dioleoyl-*sn*-glycero-3-phosphoethanolamine-N-(biotinyl) (DOPE-Biotin) in the kinesin IMA in the presence of biotinylated microtubules and streptavidin, and characterized the formation of LNTs from these vesicles (Figure 1A). The GUVs also included 0.5% Texas Red, 1,2-dihexadecanoyl-*sn*-glycero-3-phosphoethanolamine (Texas Red-DHPE) to permit characterization of LNT formation by fluorescence microscopy. Figure 1B shows an example of the formation of LNTs from this lipid formation. At 140 s, two GUVs were visible in the field of view and driven together by the gliding microtubules (not visible in these images) at 230 s (Figure 1B). Biotin-streptavidin-biotin bonding between the GUVs subsequently lead to formation of an LNT (approximately 3.5 μm in length) between the two GUVs (260 s), as well as extrusion of a second, longer (19.8 μm) LNT without destroying the parent GUVs (600 s; Figure 1B). The process of LNT extrusion may continue until the ATP in the system has been depleted, or aggregation of microtubules via biotin-streptavidin binding limits motility. Observation of network formation in this system suggested that LNT formation followed a predictable, two-step process in which (*i*) transport of GUVs lead to collisions among and aggregation of GUVs, and (*ii*) extrusion of LNTs from the parent vesicles based on microtubules acting on the aggregate in opposing direction, providing an opposing force for LNT formation (Supplementary Figure 1). In the case of MLVs, there are numerous layers of lipid bilayers within the vesicle, which enables extrusion of LNTs from a single vesicle. Conversely, GUVs typically contain one or two bilayers within a vesicle, which makes extrusion of nanotubes from a single vesicle less frequent. Therefore, we speculate that the aggregation of GUVs by microtubules enables the formation of LNTs because the reservoir of usable lipid increases as GUVs assemble into an aggregate. This proposed mechanism is consistent with observations reported in other systems in which aggregation of GUVs is also required for nanotube formation.[26-28]

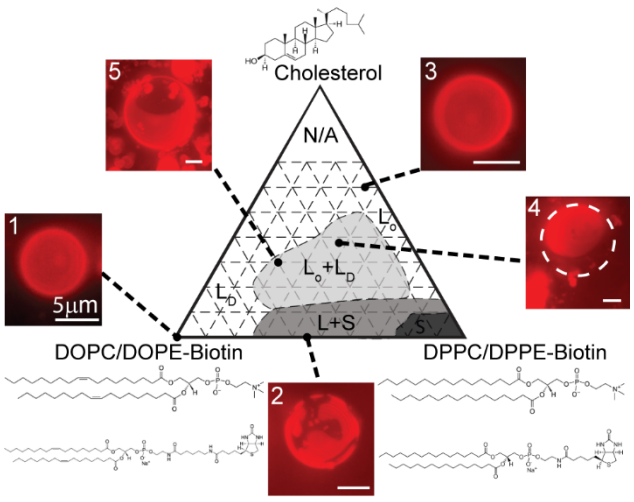

Figure 2. Phase Diagram of Lipid Mixtures. Adapted from the well-studied DOPC/DPPC/Cholesterol lipid mixture,[13] we formed GUVs for the five lipid formulations used in this study and confirmed their phase behavior. (1) 95% DOPC, 5% DOPE-Biotin. Single liquid phase (L_D) (2) 50% DOPC, 45% DPPC, 5% DOPE-Biotin. Liquid-Solid phase (L_D-S) (3) 60% Cholesterol, 35% DPPC, 5% DOPE-Biotin. Single liquid-ordered phase (L_O) (4) 19% DOPC, 38% DPPC, 38% Cholesterol, 5% DOPE-Biotin. Liquid-liquid coexistence (L_O-L_D) (5) 45% DOPC, 20% DPPC, 30% Cholesterol, 5% DOPE-Biotin. Liquid-liquid coexistence (L_O-L_D). All scale bars corresponded to 5 μm. Texas Red-DHPE was used to label the lipid membranes (0.5%) for all GUVs shown here.

One advantage of using GUVs for formation of LNTs, as opposed to MLVs, is that the compositions may be readily altered to study lipid membrane phase behavior;[29, 30] specifically, LNTs composed of different lipid phases may be formed using multi-component lipid formulations. Phase separation is the temperature dependent process of lipid membranes wherein the membrane segregates into regions of distinct lipid composition based on the physical chemistry of the phospholipid head and hydrocarbon tail groups of the component lipids. Here, we used the well-studied DOPC/DPPC (1,2-dipalmitoyl-*sn*-glycero-3-phosphocholine)/cholesterol phase diagram (Figure 2) as a guide to synthesize GUVs containing biotinylated lipids to create LNTs derived from multi-component lipid formulations.[13] GUVs were formed using an agarose gel rehydration method.[31, 32] Briefly, lipids dissolved in chloroform were spread and

dried on a 1% agarose film and then placed under vacuum for at least 2-h before rehydration. The agarose gel and lipid layer were rehydrated in osmotically balanced sucrose solution at 50°C for 1-h, and GUVs were then collected. Multiple GUV formulations were used to confirm the phase behavior of the vesicles synthesized from the agarose gel method. For imaging, all GUV formulations were synthesized with a trace amount, 0.5%, of the labeled lipid Texas Red DHPE, which strongly partitions to fluid phases.[33]

As expected, GUVs comprised entirely of unsaturated lipids, 95% DOPC and 5% DOPE-Biotin created vesicles consisting of a single liquid phase (L_D) (Figure 2). We then synthesized GUVs comprised of 60% Cholesterol, 35% DPPC, and 5% DOPE-Biotin, which created a single liquid phase (L_O) because of the presence of cholesterol in the formulation. Cholesterol is known to fluidize saturated lipids enabling the formation of liquid phases in lipid membranes without unsaturated lipids present.[13] Solid-liquid, phase-separated (L_D-S PS) GUVs were formed using a mixture of 50% DOPC, 45% DPPC, and 5% DOPE-Biotin. As expected, clear markers of liquid-solid phase separation were observed by fluorescence microscopy: irregular edges at the phase boundary between the solid phase (dark) and liquid phase (red; Figure 2).

Forming GUVs with a ternary mixture of cholesterol, unsaturated lipids, and saturated lipids within a specific region of the phase diagram, results in the coexistence of two liquid phases within the lipid membrane. Here, we examined two lipid formulations that are known to separate into coexisting liquid-ordered and the liquid-disordered phases (L_O-L_D PS). The first formulation consisted of 19% DOPC, 38% DPPC, 38% Cholesterol, and 5% DOPE-Biotin, and exhibited clear phase separation under observation by fluorescence microscopy. A smooth phase boundary between the liquid-disordered phase (L_D) (red) and the liquid-ordered phase (L_O) (dark) indicating liquid-liquid coexistence was clearly visible under fluorescence microscopy (Figure 2). Notably, in this formulation the L_D phase was the minority phase in

the membrane, which was expected as only 24% of the lipids in the formulation should strongly partition into the L_D phase. The second formulation investigated consisted of 45% DOPC, 20% DPPC, 30% cholesterol, 5% DOPE-Biotin, and exhibited phase separation (Figure 2). Again, a smooth boundary between the two phases was observed, indicating the coexistence of two liquid phases on the GUV lipid membrane. In this formulation, however, the majority phase observed on the vesicle membrane was the L_D phase (red) because 50% of the lipids used in the formulation, strongly partition to the L_D phase.

LNTs Networks Extruded from Multi-Lipid Component and Multi-Phase GUV Formulations.

The ability of multi-lipid/multi-phase GUVs to support the formation of LNT networks in the kinesin gliding motility assay was evaluated by first examining LNTs extruded from L_D-S PS GUVs composed of 50% DOPC, 45% DPPC, and 5% DOPE-Biotin. Here, the LNTs formed from these GUVs (Figure 3A) were qualitatively similar to the LNTs observed for the 95% DOPC, 5% DOPE-Biotin formulation (Figure 1) as indicated by the multiple junctions and branches between LNTs in the networks. We then examined the networks extruded from the L_O-L_D PS GUVs (Figure 3B, C). The LNTs derived from these GUVs were also similar to the networks extruded from the L_D-S PS GUVs and L_D GUVs. Notably, the functional lipid in these three formulations, DOPE-Biotin, partitions strongly to disordered and liquid phases due to its two oleoyl hydrocarbon tails.[34, 35] As such, the LNTs extruded from these vesicles were likely compositionally composed of lipids that partition into the L_D phase. Moreover, the similarities between the LNTs derived from these different GUV formulations were likely related to being primarily composed of unsaturated lipids. Additionally, the nanotubes extruded from these GUVs were of similar lengths. Specifically, the average length of a nanotube was 53.8 ± 9.8 μm (mean ± 95%CI), 55.8 ± 9.4 μm, 59.9 ± 16.4 μm, and 53.2 ± 9.2 μm for the 95% DOPC GUVs, L_D-S PS GUVs, 24% unsaturated L_O-L_D PS GUVs, and 50% unsaturated L_O-L_D PS GUVs respectively. These lengths are similar to those reported for tunneling nanotubes between cells, which can reach lengths up to 200 μm.[36] In contrast to tunneling nanotubes,

LNTs extruded from multi-lipid/multi-phase GUVs exhibit significant branching and interconnectedness, reminiscent of the ER and Golgi apparatus. Prior studies on LNTs from MLVs suggest that the relative length and frequency of branching may be tuned by varying the surface density of microtubules, or changing the membrane composition of the parent vesicles.[21, 24] Collectively, these data indicated that LNTs may be extruded from L_D GUVs and were morphologically similar regardless of composition.

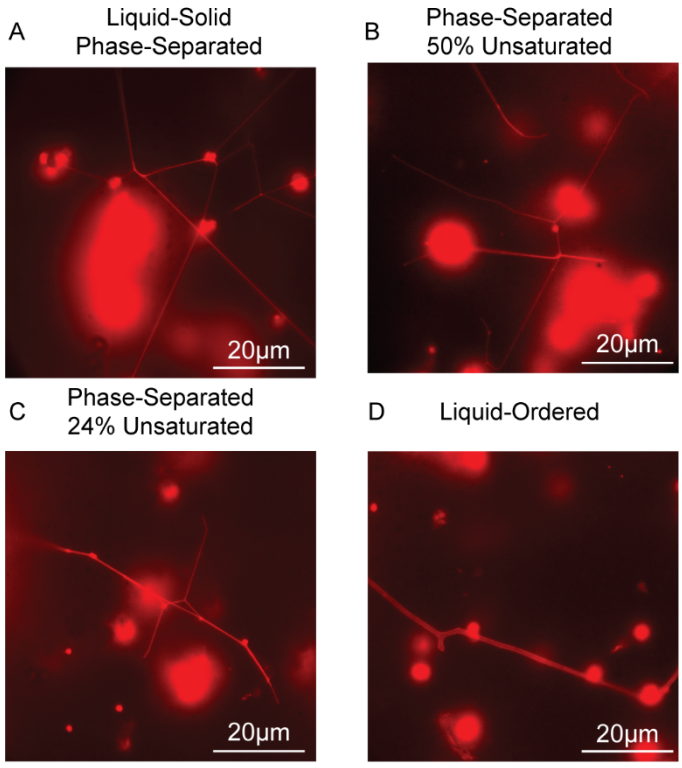

Figure 3. Lipid Nanotube Networks Formed by Multi-Component Lipid Membranes. Fluorescence images of lipid nanotube networks derived from Liquid-Solid Phase-Separated (L_D-S) GUVs (A), Phase-Separated GUVs containing 50% unsaturated lipid (50% unsaturated L_O-L_D PS) (B), Phase-Separated GUVs containing 24% unsaturated lipid (24% unsaturated L_O-L_D PS) (C), and liquid-ordered (L_O) phase GUVs (D). All scale bars corresponded to 20 μm. Lipid membranes were labeled with 0.5% Texas Red-DHPE.

Formation of LNTs from the GUV formulation, 60% Cholesterol 35% DPPC, 5% DOPE-Biotin was examined next to address the question as to whether L_O phases could support LNT extrusion. Qualitative

differences were observed between these LNTs (Figure 3D) and the LNTs formed from the L_D GUV formulation (i.e., 95% DOPC, 5% DOPE-Biotin; Figure 1). Most notably, the LNTs exhibited less branching, forming predominantly straight LNTs with infrequent, small branches. Further, the average length of extruded nanotubes from the L_O formulation was 34.9 ± 7.8 μm. When compared with the L_D lengths (50-60 μm), a significant difference between the length of L_D and L_O phases was observed via a one-way ANOVA test ($p<0.05$) (Supplementary Figure 2). LNTs formed from the L_O GUVs were also noticeably thicker than those formed from L_D formulations. To quantify this observation, the diameter of LNTs were measured from binary images of the LNTs formed from each GUV formulation (see Experimental section for details). Here, LNTs derived from unsaturated lipids (L_D GUVs and domains) all had similar LNT diameters of 6-7 pixels. In contrast, LNTs derived from the L_O GUV formulation were 16-18 pixels in diameter, significantly (ca. 2.6-times) larger than the tubes extruded from the L_D formulation ($P<0.05$; Supplementary Figure 3). The diameters of extruded L_D and L_O tubes have been previously estimated to be 60 and 110 nm, respectively.[20] The larger diameter observed for the L_O formulation was a direct consequence of the composition of the parent GUV. Specifically, the 60% cholesterol formulation contained a majority fraction of saturated lipid (35% DPPC) and very small molar fraction of unsaturated lipids (5% DOPE-Biotin), which resulted in thicker LNTs. The observed difference in diameter was consistent with previous work that determined that saturated lipids form thicker LNTs when compared to unsaturated lipids, owing to their larger bending modulus and higher rigidity.[20, 22, 37, 38] The diameter values of synthetic LNTs are also consistent those reported for biological tubules including those of the ER and Golgi apparatus (30-50 nm),[39, 40] as well as tunneling nanotubes (50-1000 nm).[41]

Multi-Component Lipid Nanotubes Contain Enriched Nodes.

The observations for LNTs extruded from multi-phase GUVs raised questions as to whether (*i*) LNTs could be extruded from the L_O phase of phase-separated GUVs, and (*ii*) whether phase separation could

occur in LNTs. To address these questions, we prepared phase-separated GUV formations containing both 3% DOPE-Biotin (partitions to the L_D phase) and 2% 1,2- dipalmitoyl-*sn*-glycero-3-phosphoethanolamine-N-(bio-tinyl) (DPPE-Biotin) (partitions to the L_O phase),[34, 35] which enabled LNT extrusion from both the L_D and L_O phase. Additionally, the GUVs were labeled with both Oregon Green DHPE (0.5%) and Texas Red DHPE (0.5%), enabling visualization of the L_O phase and L_D phase, respectively. [42]

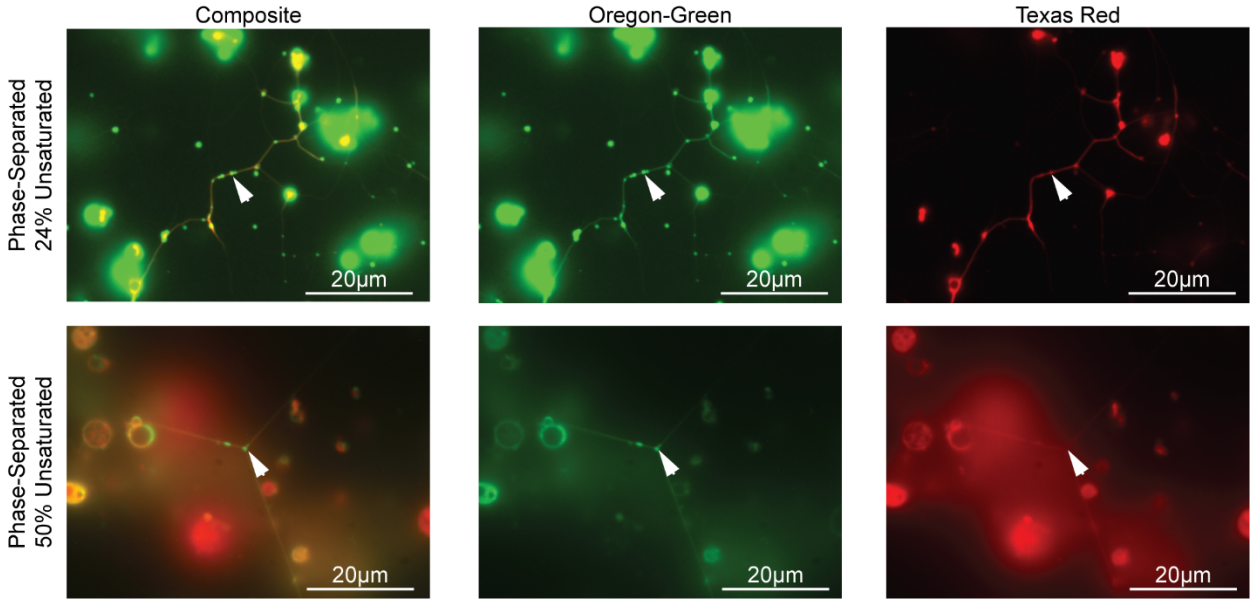

Figure 4. Lipid Nanotubes Contain Nodes Enriched in Lipids. Composite, Green Channel, and Red Channel fluorescence images of nanotubes derived from phase-separated 24% unsaturated (top) and 50% unsaturated (bottom) GUVs. In both formulations it appeared that these nodes were brighter in the Green channel than the red channel. Specifically, in the phase-separated 50% unsaturated network these nodes appeared only in the Green Channel. Lipids were labeled with 0.5% Oregon Green-DHPE and Texas Red-DHPE. Scale bars correspond to 20 μm.

LNT networks were readily formed from phase-separated 24% unsaturated GUVs containing both DPPE-Biotin and DOPE-Biotin (Figure 4). In these two-color images, the LNTs clearly exhibited both red and green fluorescence, which suggested co-existence of the saturated and unsaturated lipids. In addition,

nodes (i.e., bright dots) were observed along the length of the LNTs. Here, we observed the enrichment (i.e. stronger green fluorescence signal compared to the signal in the LNT) of Oregon Green fluorescence in these nodes suggesting that these nodes along the LNT were primarily composed of saturated lipids. Specifically, while the LNTs had similar intensities, the nodes exhibited a stronger green fluorescence signal. Similar results were obtained using the GUV formulation containing 50% unsaturated lipids (Figure 4). LNT networks were readily formed, and enrichment of Oregon Green lipids was observed in nodes. When observing the LNTs and nodes in the red channel, however, it was noted that Texas Red DHPE had been excluded from the node. This result suggested that phase-separation occurred along the LNT and that these nodes were enriched in saturated lipid. Furthermore, this result suggested that these regions within the LNTs were likely enriched in the L_O.

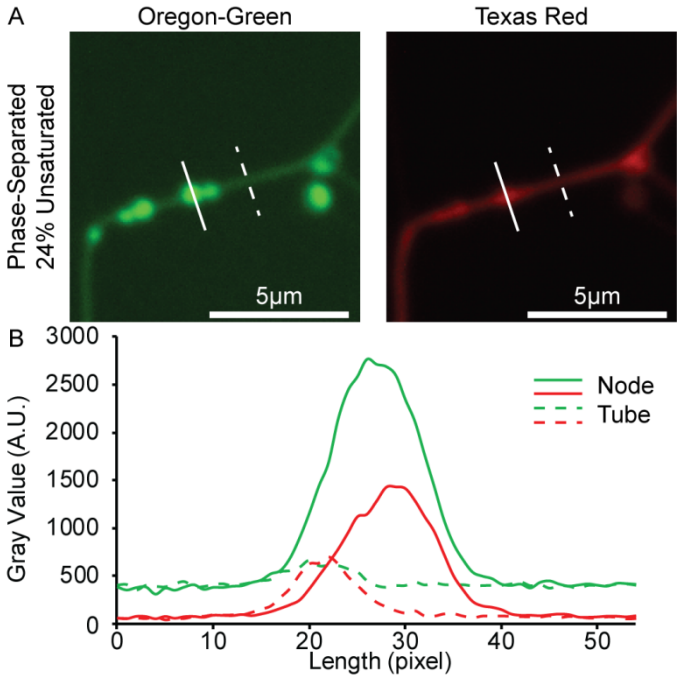

Figure 5. Quantifying lipid partitioning within nodes. (A) Green (left) and Red (right) channel images of the lipid nanotube network derived from phase-separated 24% unsaturated GUVs from Figure 4. Line profiles of the fluorescence intensity of the node (solid line) and tube (dashed line) were then taken. (B) The line profiles of

fluorescence intensity (Gray Value) of the node (solid) and tube (dashed) for each channel (Green and Red) plotted. Peaks corresponded to the labeled membrane. Scale bars corresponded to 5 μm.

L_O Lipids Partition Strongly into Nodes within LNT Networks.

Enrichment of lipids at nodes along the LNTs was next quantified by calculating the ratio of the background subtracted maximum grey value (a.u.) of the node to the background subtracted maximum grey value (a.u.) of the LNT. As an example, close examination of the network formed by 24% unsaturated L_O-L_D PS GUVs (Figures 4 and 5A) exhibited a noticeable difference in partitioning for the node in both channels. In both channels, the node was clearly more enriched in labeled lipids in comparison to the fluorescence observed in the LNT (Figure 5A). By calculating the ratio of the fluorescence of the node to the fluorescence of the LNT in the green channel, we observed that the node is approximately nine-times brighter than parent LNT (Figure 5B). In contrast, when this ratio was calculated for the same node and LNT in the red channel, we observed that that the node was approximately two-fold brighter than the parent LNT (Figure 5B). Overall, these data suggested that nodes were enriched in both saturated and unsaturated lipids. However, the high level of partitioning of the Oregon Green-DHPE lipids in the nodes suggests that the nodes were more enriched in saturated lipids than unsaturated lipids.[42] For the 24% unsaturated L_O-L_D PS formulation, the ratios in the green and red channels were 18.5 ± 2.3 (95% CI) and 4.5 ± 0.7, respectively (n = 191) (Supplementary Figure 4). For the 50% unsaturated L_O-L_D PS formulation, the ratios in the green and red channels were 13.3 ± 4.8 and 2.6 ± 0.6, respectively (n = 58) (Supplementary Figure 5).

Collectively, the results shown in Figures 4 and 5 demonstrated that these nodes were likely composed primarily of saturated lipids in the L_O phase. It has been previously hypothesized that there are regions on cellular membranes that are enriched in cholesterol and saturated lipids and involved in spatial and

temporal organization of membrane proteins.[15, 16, 43, 44] The nodes in our model system may serve as a platform for characterizing the preferred lipid environment for membrane proteins organization. Furthermore, regions enriched in cholesterol and saturated lipids have also been observed in the ER and Golgi apparatus.[45, 46] Thus, the formation of such regions in our synthetic LNTs opens the door to potentially mimic biologically relevant lipid organization in *ex vivo,* synthetic systems.

Lipid Nanotube Networks Extruded by Multi-Component GUVs Demonstrate Liquid-Liquid Phase Coexistence.

L_O-L_D PS GUVs were prepared with 5% DPPE-Biotin, which is known to moderately partition into the L_O phase with a partitioning factor ranging from 1.1[34] to 1.4.[35] As such, we expected to observe thick, L_O LNTs and thin L_D LNTs in networks formed from these GUVs. Indeed, both thick and thin LNTs (Figure 6A) were extruded from 24% unsaturated L_O-L_D PS GUVs labeled with 0.5% Oregon Green DHPE. Note that because both Oregon Green-DHPE and DPPE-Biotin partition more strongly to the L_O phase, we see a low green signal for the thin L_D tubes (Figure 6A inset). We also observed the coexistence of L_O and L_D nanotubes in the 50% unsaturated L_O-L_D PS formulation (Supplementary Figure 7). Phase-separation within LNTs was also clearly observed, demonstrating that both the L_O and L_D phases could coexist within the same LNTs, similar their phase coexistence behavior observed in GUVs (Figure 6B; Supplementary Figure 6). This result was rather interesting as LNTs are highly curved membrane structures, and coexistence of different phase may not intuitively be expected.

Previous work has demonstrated that lipids in the L_O phase localize in low curvature geometries, indicating that these LNTs are within a critical membrane curvature threshold that enables phase separation.[47-50] The appearance of phase-separated domains along the LNTs may be explained by its intrinsic dimensionality. Specifically, LNTs are one-dimensional structures and experience high curvature

in only one dimensions, as compared small vesicles in which lipids experience high curvature in two dimensions. Work done by Brewster and Safran demonstrated that increasing the concentration of cholesterol in DOPC and DPPC membranes increased the size of phase-separated domains.[50] Therefore, the appearance of phase-separated domains within the LNTs in our studies may also be explained by the large presence of cholesterol (>30%) in our lipid formulation, which has also been seen in a previous extruded lipid nanotube system.[20] Additionally, lipid membrane phase separation has also been observed in highly curved mitochondrial membranes during apoptosis and energy flux processes.[51]

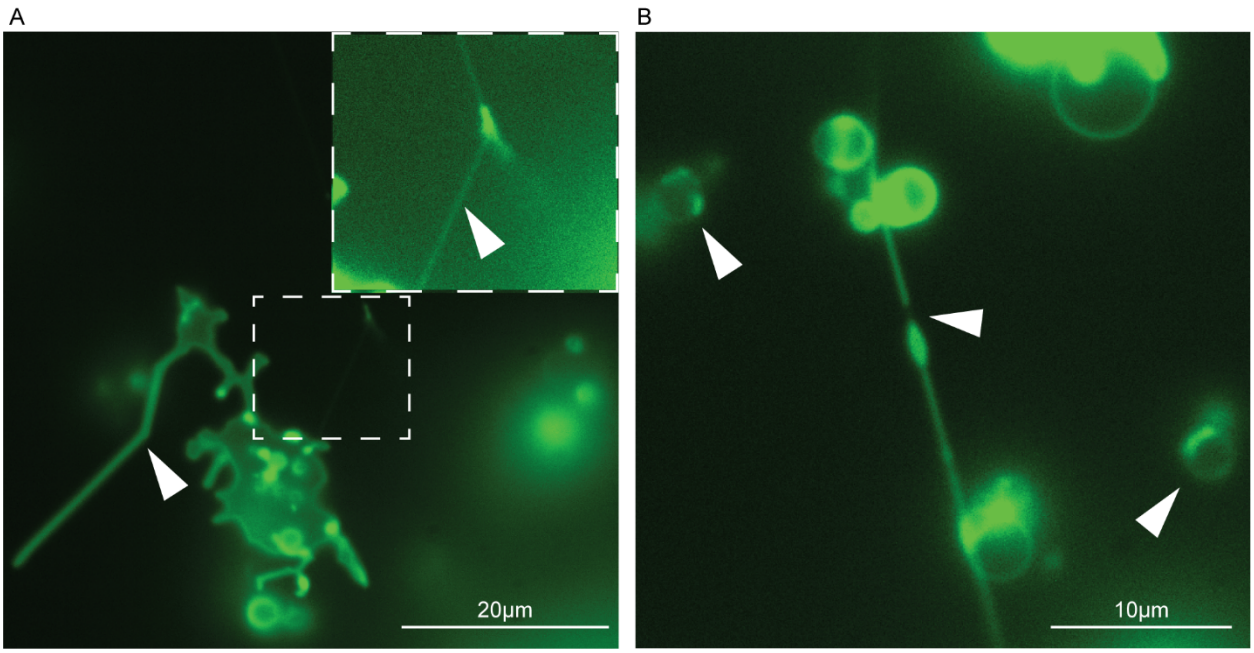

Figure 6. Nanotube Networks formed by DPPE-Biotin Lipids contain coexisting L_O and L_D nanotubes. (A) Fluorescence image demonstrating the formation of L_O and L_D (inset) tubes from the same parent GUV. Scale bar corresponded to 20 μm. (B) Fluorescence image of phase-separation within a lipid nanotube. Note the phase-separation in not extruded GUVs in the field of view. Scale bar corresponded to 10 μm. The lipid membranes were labeled with a trace amount of OG-DHPE (0.5%).

Conclusion

Overall, our work demonstrates the ability to form complex LNT networks from GUVs and establishes a model system for further studying lipid phase separation in LNTs. Lipid membrane phase separation in liposomes has been a powerful tool used to achieve improved functionality in man-made drug delivery systems[52] and has been hypothesized to help organize proteins and lipids spatially and temporally in living systems.[15, 16] Future application of our system combined with the ability to achieve phase-separation in LNTs opens the door to developing more complex and functional synthetic LNT networks for studying cell communication, nanofluidic transport of biomolecules, transmembrane protein lipid preferences, and development of synthetic neuronal networks.

Experimental

Chemical Reagents

PIPES (Piperazine-N,N'-bis(2-ethanesulfonic acid)), MgCl2, EGTA, KOH, GTP, paclitaxel (Taxol), casein, AMP-PNP (β,γ-imidoadenosine 5'-triphosphate), ATP(Adenosine 5'-triphosphate disodium salt), glucose oxidase, catalase, D-glucose, 6-hydroxy-2,5,7,8-tetramethylchroman-2-carboxylic acid, DTT, chloroform, and Trolox were purchased from Sigma-Aldrich. Unlabeled, HiLyte 488, and biotin-labeled lyophilized porcine brain tubulin were purchased from Cytoskeleton. 1,2-Dioleoyl-sn-glycero-3-phosphocholine (DOPC), 1,2-dipalmitoyl-sn-glycero-3-phosphocholine (DPPC), cholesterol (ovine wool),1,2-dioleoyl-sn-glycero-3-phosphoethanolamine-N-(bio-tinyl) (DOPE-Biotin), and 1,2- dipalmitoyl-sn-glycero-3-phosphoethanolamine-N-(bio-tinyl) (DPPE-Biotin) were purchased from Avanti Polar Lipids. Texas Red, 1,2-dihexadecanoyl-sn-glycero-3-phosphoethanolamine (TR-DHPE) and Oregon Green, 1,2-dihexadecanoyl-sn-glycero-3-phosphoethanolamine (OG-DHPE) were purchased from Invitrogen.

Microtubule Preparation

For HiLyte488 labeled microtubules, HiLyte™ Fluor 488-labeled, biotin-labeled and unlabeled tubulin in a 1:1:6 molar ratio was suspended in BRB80 buffer (80 mM PIPES, 1 mM $MgCL_2$, and 1 mM EGTA adjusted to pH 6.9 with KOH) containing 1 mM GTP at a concentration of 16 µM and then polymerized for 30 minutes at 37°C, while microtubules made without HiLyte488 tubulin were made at a 1:7 biotin labeled to unlabeled tubulin ratio. After polymerization microtubules were stabilized by diluting to 0.8 µM with BRB80T, BRB80 buffer containing 1 µM paclitaxel. All samples were stored at room temperature.

GUV Preparation

Giant unilamellar vesicles (GUVs) were formed by following published protocols using agarose coated microscope coverslips.[31, 32] The lipid compositions used in this study were based on the well-studied DOPC/DPPC/Cholesterol ternary lipid formulation. Lipids dissolved in chloroform were spread on agarose coated coverslips and placed under vacuum for at least 2 h to remove all the solvent. The lipid film was rehydrated in sucrose solution (575 mOsm) at approximately 50°C to exceed the expected melting temperature of DPPC, 41°C. In all experiments vesicle solution osmolarity was measured using a vapor pressure osmometer (Advanced Instruments). All samples were stored at 4°C.

Motility Assay

A 5 mm x 20 mm x 0.450 mm flow cell was created on a glass slide using double-sided tape and a glass coverslip. The motor protein kinesin (KIF5B) was used to immobilize microtubules to the coverslip surface for imaging. Kinesin was expressed and purified using established protocols. The flow cell was filled with 1mM kinesin in the buffer BRB80CAT, BRB80 buffer containing 0.2 mg mL^{-1} casein, 1mM ATP, 1 µM paclitaxel, and 1 mM Trolox. After a 5-min incubation, 20 µL of the microtubule solution was introduced into the channel. Following another 5-minute incubation, the channel was washed with

imaging solution, BRB80 buffer containing, 0.2 mg mL^{-1} casein, 1mM ATP, 1 µM paclitaxel, 1mM Trolox, 0.02 mg mL^{-1} glucose oxidase, 0.008 mg mL^{-1} catalase, 20 mM D-glucose, and 1 mM DTT.

Lipid Nanotube Network Fabrication

After microtubules were introduced into the flow cell, streptavidin diluted to 0.01 mg mL^{-1} in imaging solution was introduced into the channel and incubated for 10 minutes. The channel was then washed with imaging solution and GUVs diluted in motility solution was added to the flow chambers and immediately imaged on the microscope. For time course images, the chamber was sealed with Velap and images were taken every ten minutes for an hour to capture the formation of LNTs. For single images to capture completed LNTs, a 30-minute timer was started and at the end of this time period, 2 µL of 100 mM AMP-PNP was added to the flow cell to inhibit microtubule motility and preserve the properties of the LNT. All experiments were conducted at room temperature.

Fluorescence Microscopy

Fluorescence imaging was performed on an IX-81 Olympus microscope with 100X/1.4 Numerical Aperature oil immersion objective, Semrock Brightline Pinkel DA/FI/TR/Cy5/Cy7-5X-A000 filter set, 3.0 ND filter, and Orca Flash 4.0 digital camera. The lipid nanotube network fabrication time course images were acquired at 10 second intervals for a total duration of 10 minutes.

LNT Diameter Measurements

Fluorescence images were converted into binary images using the threshold feature of ImageJ. Pixels above the threshold were converted to a 0 value while beneath this threshold the pixels were converted

to a 255 value. A rectangle of known length (50 or 100 pixels) was drawn over a specified tube. The sum of the pixel intensities (integrated density) of this region of interest (ROI) was taken. Then area of pixels in the tube was determined by dividing the integrated density by 255. To acquire the width of the tubule in pixels, the pixel area was divided by the length of the rectangle used to create the ROI.

Nodule Partitioning Measurements

ImageJ was used to analyze the images. The line profile tool was used to capture the maximum background-subtracted peak intensity of a nodule and tube in both the Texas Red and Oregon Green channels. To determine the partitioning of lipid in the nodule the background subtracted maximum gray value of the nodule was divided by the background subtracted maximum gray value of the tube.

Supporting Information

The Supporting Information is available free of charge on the ACS Publications website at DOI:

- Fluorescence images demonstrating microtubule transport of vesicles and extrusion of LNTs, detailed size comparison of LNTs formed from different phases, comparison of LNT thickness (i.e., diameter) for different phases, comparison of node brightness for 24% and 50% unsaturated phase-separated vesicles, summary table of GUV and LNT characteristics, and fluorescence images of LNTs structures formed by 24% and 50% unsaturated phase-separated vesicles

Acknowledgments

We sincerely thank Dr. Brad Jones for his critical reviews and comments during the preparation of this manuscript. This work was supported by the U.S. Department of Energy, Office of Basic Energy Sciences, Division of Materials Sciences and Engineering (BES-MSE). Kinesin synthesis and fluorescence

microscopy were performed through a user project (ZIM) at the Center for Integrated Nanotechnologies, an Office of Science User Facility operated for the U.S. Department of Energy (DOE) Office of Science. Sandia National Laboratories is a multimission laboratory managed and operated by National Technology & Engineering Solutions of Sandia, LLC., a wholly owned subsidiary of Honeywell International, Inc., for the U.S. DOE's National Nuclear Security Administration under contract DE-NA-0003525. This paper describes objective technical results and analysis. Any subjective views or opinions that might be expressed in the paper do not necessarily represent the views of the U.S. Department of Energy or the United States Government.

References

1. Rustom, A.; Saffrich, R.; Markovic, I.; Walther, P.; Gerdes, H. H., Nanotubular highways for intercellular organelle transport. *Science* **2004,** 303, (5660), 1007-1010.
2. Lippincott-Schwartz, J.; Roberts, T. H.; Hirschberg, K., Secretory protein trafficking and organelle dynamics in living cells. *Annu. Rev. Cell Dev. Biol.* **2000,** 16, 557-589.
3. Belting, M.; Wittrup, A., Nanotubes, exosomes, and nucleic acid-binding peptides provide novel mechanisms of intercellular communication in eukaryotic cells: implications in health and disease. *J. Cell Biol.* **2008,** 183, (7), 1187-1191.
4. Hurtig, J.; Chiu, D. T.; Onfelt, B., Intercellular nanotubes: insights from imaging studies and beyond. *Wiley Interdiscip. Rev. Nanomed. Nanobiotechnol.* **2010,** 2, (3), 260-76.
5. Sciaky, N.; Presley, J.; Smith, C.; Zaal, K. J.; Cole, N.; Moreira, J. E.; Terasaki, M.; Siggia, E.; Lippincott-Schwartz, J., Golgi tubule traffic and the effects of brefeldin A visualized in living cells. *J Cell Biol.* **1997,** 139, (5), 1137-55.
6. Sprong, H.; van der Sluijs, P.; van Meer, G., How proteins move lipids and lipids move proteins. *Nat. Rev. Mol. Cell Biol.* **2001,** 2, (7), 504-513.
7. Gousset, K.; Schiff, E.; Langevin, C.; Marijanovic, Z.; Caputo, A.; Browman, D. T.; Chenouard, N.; de Chaumont, F.; Martino, A.; Enninga, J.; Olivo-Marin, J. C.; Mannel, D.; Zurzolo, C., Prions hijack tunnelling nanotubes for intercellular spread. *Nat. Cell Biol.* **2009,** 11, (3), 328-U232.
8. Onfelt, B.; Nedvetzki, S.; Yanagi, K.; Davis, D. M., Cutting edge: Membrane nanotubes connect immune cells. *J. Immunol.* **2004,** 173, (3), 1511-3.
9. Vidulescu, C.; Clejan, S.; O'Connor, K. C., Vesicle traffic through intercellular bridges in DU 145 human prostate cancer cells. *J. of Cell. Mol. Med.* **2004,** 8, (3), 388-396.
10. Keenan, T. W.; Morre, D. J., Phospholipid class and fatty acid composition of golgi apparatus isolated from rat liver and comparison with other cell fractions. *Biochemistry* **1970,** 9, (1), 19-&.
11. Mehnert, W.; Mader, K., Solid lipid nanoparticles - Production, characterization and applications. *Adv. Drug Deliv. Rev.* **2001,** 47, (2-3), 165-196.
12. Cremer, P. S.; Boxer, S. G., Formation and spreading of lipid bilayers on planar glass supports. *J. Phys. Chem. B* **1999,** 103, (13), 2554-2559.

13. Veatch, S. L.; Keller, S. L., Separation of liquid phases in giant vesicles of ternary mixtures of phospholipids and cholesterol. *Biophys. J.* **2003,** 85, (5), 3074-3083.
14. Hillaireau, H.; Couvreur, P., Nanocarriers' entry into the cell: relevance to drug delivery. *Cell. Mol. Life Sci.* **2009,** 66, (17), 2873-2896.
15. Varma, R.; Mayor, S., GPI-anchored proteins are organized in submicron domains at the cell surface. *Nature* **1998,** 394, (6695), 798-801.
16. Grakoui, A.; Bromley, S. K.; Sumen, C.; Davis, M. M.; Shaw, A. S.; Allen, P. M.; Dustin, M. L., The immunological synapse: A molecular machine controlling T cell activation. *Science* **1999,** 285, (5425), 221-227.
17. Dai, J. W.; Sheetz, M. P., Membrane tether formation from blebbing cells. *Biophys. J.* **1999,** 77, (6), 3363-3370.
18. Sott, K.; Karlsson, M.; Pihl, J.; Hurtig, J.; Lobovkina, T.; Orwar, O., Micropipet writing technique for production of two-dimensional lipid bilayer nanotube−vesicle networks on functionalized and patterned surfaces. *Langmuir* **2003,** 19, (9), 3904-3910.
19. Leduc, C.; Campas, O.; Zeldovich, K. B.; Roux, A.; Jolimaitre, P.; Bourel-Bonnet, L.; Goud, B.; Joanny, J. F.; Bassereau, P.; Prost, J., Cooperative extraction of membrane nanotubes by molecular motors. *Proc. Natl. Acad. Sci. U.S.A.* **2004,** 101, (49), 17096-17101.
20. Roux, A.; Cuvelier, D.; Nassoy, P.; Prost, J.; Bassereau, P.; Goud, B., Role of curvature and phase transition in lipid sorting and fission of membrane tubules. *EMBO J.* **2005,** 24, (8), 1537-1545.
21. Bouxsein, N. F.; Carroll-Portillo, A.; Bachand, M.; Sasaki, D. Y.; Bachand, G. D., A continuous network of lipid nanotubes fabricated from the gliding motility of kinesin powered microtubule filaments. *Langmuir* **2013,** 29, (9), 2992-9.
22. Döbereiner, H., Properties of giant vesicles. *Curr. Opin. Colloid Interface Sci.* **2000,** 5, (3-4), 256-263.
23. Sens, P.; Johannes, L.; Bassereau, P., Biophysical approaches to protein-induced membrane deformations in trafficking. *Curr. Opin. Cell Biol.* **2008,** 20, (4), 476-82.
24. Paxton, W. F.; Bouxsein, N. F.; Henderson, I. M.; Gomez, A.; Bachand, G. D., Dynamic assembly of polymer nanotube networks via kinesin powered microtubule filaments. *Nanoscale* **2015,** 7, (25), 10998-1004.
25. van Meer, G.; Vaz, W. L. C., Membrane curvature sorts lipids. *EMBO Rep* **2005,** 6, (5), 418-419.
26. Liu, H.; Bachand, G. D.; Kim, H.; Hayden, C. C.; Abate, E. A.; Sasaki, D. Y., Lipid nanotube formation from streptavidin-membrane binding. *Langmuir* **2008,** 24, (8), 3686-9.
27. Davidson, M.; Karlsson, M.; Sinclair, J.; Sott, K.; Orwar, O., Nanotube−vesicle networks with functionalized membranes and interiors. *J. Am. Chem. Soc.* **2003,** 125, (2), 374-378.
28. Evans, E.; Bowman, H.; Leung, A.; Needham, D.; Tirrell, D., Biomembrane templates for nanoscale conduits and networks. *Science* **1996,** 273, (5277), 933-935.
29. Wesolowska, O.; Michalak, K.; Maniewska, J.; Hendrich, A. B., Giant unilamellar vesicles - a perfect tool to visualize phase separation and lipid rafts in model systems. *Acta Biochim. Pol.* **2009,** 56, (1), 33-39.
30. Veatch, S. L.; Polozov, I. V.; Gawrisch, K.; Keller, S. L., Liquid domains in vesicles investigated by NMR and fluorescence microscopy. *Biophys. J.* **2004,** 86, (5), 2910-2922.
31. Greene, A. C.; Henderson, I. M.; Gomez, A.; Paxton, W. F.; VanDelinder, V.; Bachand, G. D., The role of membrane fluidization in the gel-assisted formation of giant polymersomes. *PLoS One* **2016,** 11, (7), 13.
32. Horger, K. S.; Estes, D. J.; Capone, R.; Mayer, M., Films of agarose enable rapid formation of giant liposomes in solutions of physiologic ionic strength. *J. Am. Chem. Soc.* **2009,** 131, (5), 1810-9.
33. Skaug, M. J.; Longo, M. L.; Faller, R., The impact of Texas Red on lipid bilayer properties. *J. Phys. Chem. B* **2011,** 115, (26), 8500-8505.

34. Momin, N.; Lee, S.; Gadok, A. K.; Busch, D. J.; Bachand, G. D.; Hayden, C. C.; Stachowiak, J. C.; Sasaki, D. Y., Designing lipids for selective partitioning into liquid ordered membrane domains. *Soft Matter* **2015,** 11, (16), 3241-3250.
35. Honigmann, A.; Sadeghi, S.; Keller, J.; Hell, S. W.; Eggeling, C.; Vink, R., A lipid bound actin meshwork organizes liquid phase separation in model membranes. *eLife* **2014,** 3, e01671.
36. Dupont, M.; Souriant, S.; Lugo-Villarino, G.; Maridonneau-Parini, I.; Vérollet, C., Tunneling Nanotubes: Intimate Communication between Myeloid Cells. *Front. Immunol.* **2018,** 9, 43-43.
37. Leduc, C.; Campas, O.; Joanny, J. F.; Prost, J.; Bassereau, P., Mechanism of membrane nanotube formation by molecular motors. *Biochim. Biophys. Acta* **2010,** 1798, (7), 1418-26.
38. Karlsson, M.; Sott, K.; Davidson, M.; Cans, A. S.; Linderholm, P.; Chiu, D.; Orwar, O., Formation of geometrically complex lipid nanotube-vesicle networks of higher-order topologies. *Proc. Natl. Acad. Sci. U.S.A.* **2002,** 99, (18), 11573-11578.
39. Schwarz, D. S.; Blower, M. D., The endoplasmic reticulum: structure, function and response to cellular signaling. *Cell. Mol. Life Sci.* **2016,** 73, (1), 79-94.
40. Mollenhauer, H. H.; Morre, D. J., The tubular network of the Golgi apparatus. *Histochem. Cell Biol.* **1998,** 109, (5-6), 533-43.
41. Austefjord, M. W.; Gerdes, H. H.; Wang, X., Tunneling nanotubes: Diversity in morphology and structure. *Commun. Integr. Biol.* **2014,** 7, (1), e27934.
42. Bordovsky, S. S.; Wong, C. S.; Bachand, G. D.; Stachowiak, J. C.; Sasaki, D. Y., Engineering lipid structure for recognition of the liquid ordered membrane phase. *Langmuir* **2016,** 32, (47), 12527-12533.
43. Eggeling, C.; Ringemann, C.; Medda, R.; Schwarzmann, G.; Sandhoff, K.; Polyakova, S.; Belov, V. N.; Hein, B.; von Middendorff, C.; Schonle, A.; Hell, S. W., Direct observation of the nanoscale dynamics of membrane lipids in a living cell. *Nature* **2009,** 457, (7233), 1159-U121.
44. Zacharias, D. A.; Violin, J. D.; Newton, A. C.; Tsien, R. Y., Partitioning of lipid-modified monomeric GFPs into membrane microdomains of live cells. *Science* **2002,** 296, (5569), 913-916.
45. Brugger, B.; Sandhoff, R.; Wegehingel, S.; Gorgas, K.; Malsam, J.; Helms, J. B.; Lehmann, W. D.; Nickel, W.; Wieland, F. T., Evidence for segregation of sphingomyelin and cholesterol during formation of COPI-coated vesicles. *J. Cell Biol.* **2000,** 151, (3), 507-517.
46. Bagnat, M.; Keranen, S.; Shevchenko, A.; Shevchenko, A.; Simons, K., Lipid rafts function in biosynthetic delivery of proteins to the cell surface in yeast. *Proc. Natl. Acad. Sci. U.S.A.* **2000,** 97, (7), 3254-3259.
47. Parthasarathy, R.; Yu, C. H.; Groves, J. T., Curvature-modulated phase separation in lipid bilayer membranes. *Langmuir* **2006,** 22, (11), 5095-9.
48. Sadeghi, S.; Muller, M.; Vink, R. L., Raft formation in lipid bilayers coupled to curvature. *Biophys. J.* **2014,** 107, (7), 1591-600.
49. Iglic, A.; Hagerstrand, H.; Veranic, P.; Plemenitas, A.; Kralj-Iglic, V., Curvature-induced accumulation of anisotropic membrane components and raft formation in cylindrical membrane protrusions. *J. Theor. Biol.* **2006,** 240, (3), 368-373.
50. Brewster, R.; Safran, S. A., Line active hybrid lipids determine domain size in phase separation of saturated and unsaturated lipids. *Biophys. J.* **2010,** 98, (6), L21-3.
51. Epand, R. F.; Tokarska-Schlattner, M.; Schlattner, U.; Wallimann, T.; Epand, R. M., Cardiolipin clusters and membrane domain formation induced by mitochondrial proteins. *J. Mol. Biol.* **2007,** 365, (4), 968-980.
52. Imam, Z. I.; Kenyon, L. E.; Ashby, G.; Nagib, F.; Mendicino, M.; Zhao, C.; Gadok, A. K.; Stachowiak, J. C., Phase-separated liposomes enhance the efficiency of macromolecular delivery to the cellular cytoplasm. *Cell. Mol. Bioeng.* **2017,** 10, (5), 387-403.

TOC Image & Description

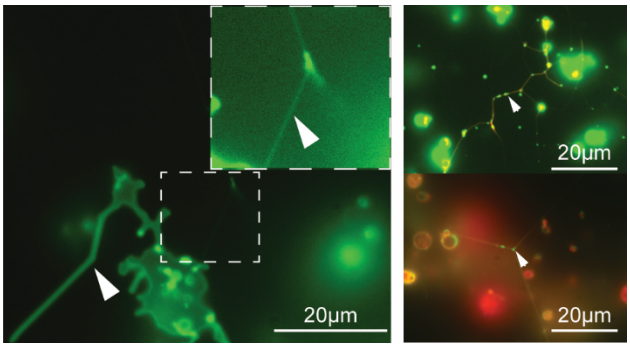

Explored the kinesin motor-driven formation of lipid nanotube (LNT) networks from multi-component phase-separated giant unilamellar vesicles (GUVs), which resulted in LNTs wherein lipids partitioned into nodes along the tubes, formed thick and thin LNTs depending on the GUV formulation used, and demonstrated phase-separation of lipids within LNTs.